Available online at www.sciencedirect.com

SCIENCE DIRECT®

Journal of the European Ceramic Society 24 (2004) 2847–2851

www.elsevier.com/locate/jeurceramsoc

Mechanical and erosion-resistance properties of slag α-sialon ceramics

Wei-Wu Chen[a], Joseph Steel[b], Yu Zhang[b], Jiu-Xin Jiang[a], Yi-Bing Cheng[b], Pei-Ling Wang[a,*], Dong-Sheng Yan[a]

[a]*The State Key Lab of High Performance Ceramics and Superfine Microstructure, Shanghai Institute of Ceramics, CAS, Shanghai 200050, PR China*

[b]*School of Physics and Materials Engineering, Monash University, Clayton, Victoria, 3800, Australia*

Received 24 August 2003; accepted 27 September 2003

Abstract

In the present work, the mechanical properties and erosion-resistance ability of hot-pressed and pressureless sintered slag α-sialon ceramics, which were started from slag α-sialon powders prepared by SHS technique based on slag powders, [J. Mater. Chem. 12 (2002) 1199] were measured. The hardness and toughness of pressureless sintered slag α-sialon samples reached 15.53 GPa and 4.72 MPam$^{1/2}$ respectively. The strength of hot-pressed slag α-sialon ceramics reached 599 MPa as well. In comparison with Al_2O_3 and ZrO_2 ceramics, as-sintered slag α-sialon ceramics showed much higher erosion-resistance ability. These properties are very close to that of normal α-sialon ceramics prepared by expensive chemical agents as raw materials.

Keywords: Erosion resistance; Mechanical properties; Sialons; Slags; Waste materials; Wear resistance

1. Introduction

Sialon ceramics [mainly α-sialon (α′) and β-sialon (β′)] exhibit great potential for engineering applications because of their excellent mechanical properties, such as high hardness, toughness and strength.[2] Typically, sialons are prepared by firing powder compacts of Si_3N_4, AlN, Al_2O_3 and some oxide sintering additives at high temperatures via a liquid phase sintering mechanism. Both the expensive starting powders and the complex manufacturing process (compared to most oxide ceramics) have limited the practical application of sialon ceramics. On the other hand, slag is a waste product from metallurgical plants and is produced on a daily basis in large quantities. Therefore, there are economical and ecological advantages for the reuse of this wasteful slag. The basic components in the blast furnace slag are CaO, SiO_2, Al_2O_3 and MgO. There have been previous attempts to produce cement and glass out of slag.[3,4] However, little literature is available on the use of slag to synthesize advanced ceramics, although its composition can be easily matched to that of the sialon ceramics if extra nitrogen is incorporated. Recently, we synthesized low-cost (Ca, Mg)-α-sialon powder from slag using a novel synthesis method, namely Self-propagating High-temperature Synthesis (SHS).[1] This process has obvious advantages in comparison to traditional Carbothermal Reduction and Nitridation (CRN) method, such as high-productivity and low-energy consumption.[5] The synthesized α-sialon powders show some good sinterability and can be densified at 1750 °C by hot-press sintering. In the present work, the mechanical properties of hot-pressed and pressure-less sintered slag-sialon ceramic samples were further studied. And as an important potential application, the erosion behaviour of slag-sialon ceramics were measured and compared with Al_2O_3, ZrO_2 and normal pressureless sintered Ca-α-sialon materials.

2. Experimental

The characters of slag α-sialon powder synthesized using SHS have been described in a previous paper.[1] This powder was ball milled to about 1 μm (shown in Fig. 1) and then sintered directly by hot pressing

---

* Corresponding author.
E-mail address: plwang@sunm.shcnc.ac.cn (P.-L. Wang).

0955-2219/$ - see front matter © 2003 Elsevier Ltd. All rights reserved.
doi:10.1016/j.jeurceramsoc.2003.09.025

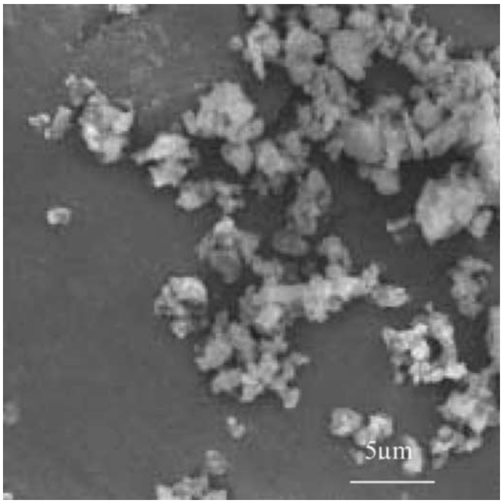

Fig. 1. SEM photo of starting slag α-sialon powder.

(1700 °C, 1 h) and pressureless sintering (1800 °C, 2 h) in a graphite furnace.

Bulk densities of the samples were measured according to the Archimedes principle. Phase identification was performed by X-ray diffraction (XRD) using a Rigaku Geigerflex diffractometer. Hardness and indentation fracture toughness were measured by using a Vickers diamond indenter under a load of 100 N for 10 s. Sintered samples were cut and ground into rectangular bar specimens (3×4×35 mm). Bending strength was measured at room temperature with an INSTRON-1195 using the three-point bending test with a span length of 30 mm and a cross-head speed of 0.5 mm/min. Morphology of the starting powder and the microstructure of solid specimens were observed under a scanning electron microscope (Jeol, JSM 840A).

The erosion tests were carried out in a gas-blast type erosion test rig, which has previously been described in detail by Zhang et al.[6] The erodent particles used were commercial grade SiC and garnet abrasive grits. The SiC particles had a size distribution between 210 and 500 μm (mean 388 μm) and the garnet particles ranged between 200 and 600 μm (mean 400 μm). The mechanical properties of the erodent particles are shown in Table 2. The test conditions were as follows: the sample-nozzle stand off distance was 13.8 mm; the particle velocity 20 m/s and the impact angle 90° or 30°. Weight loss from the target materials was tested using an analytical balance with an accuracy of 0.1 mg. Cumulative weight loss was plotted as a function of the amount of erodent impacting on the surface.

Table 1
Properties of HP- and PLS-slag-sialon samples

Samples	Measured Density (g/cm^3)	Relative density (%)	Hardness (Gpa)	Toughness (MPa·m$^{1/2}$)	Strength (MPa)
PLS	3.07	96	15.53	4.72	360
HP	3.17	99	16.02	4.48	599

Table 2
Properties of erodent particles and reference target ceramic samples

Materials	Density (g/cm^3)	Hardness (GPa)	Toughness (MPam$^{1/2}$)
Garnet	4.1	13.9	1.1
SiC	3.2	20.4	2.5
Al_2O_3	3.76	17.9	–
Mg–PSZ	5.74	9.5	13.1
Normal Ca-α-sialon (PLS)	3.2	15.6	4.5

3. Results and discussion

3.1. Mechanical properties

Ball-milled slag α-sialon powders were hot-pressed (HP) at 1700 °C for 1 h and pressureless sintered (PLS) at

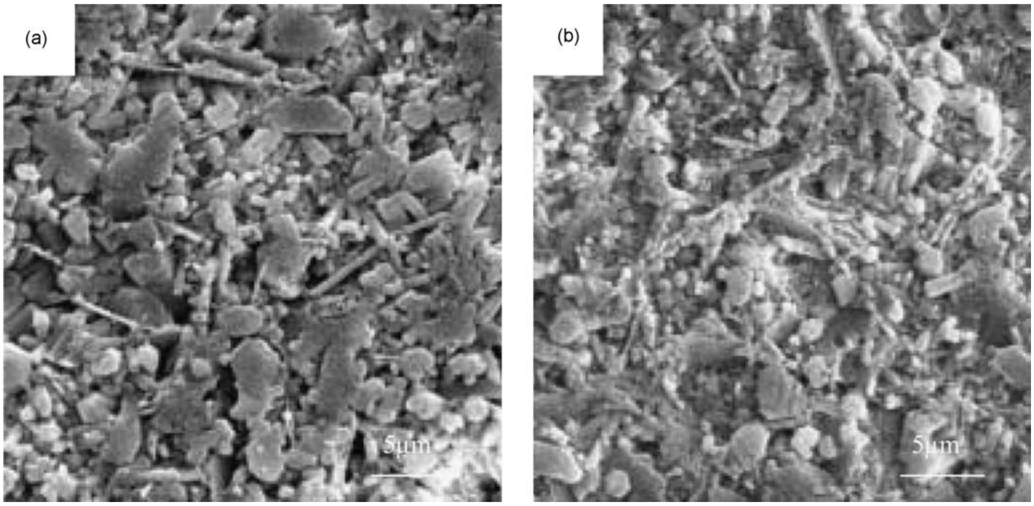

Fig. 2. Microstructure of as-sintered slag α-sialon samples (a) PLS at 1800 °C for 2 h (b) HP at 1700 °C for 1 h.

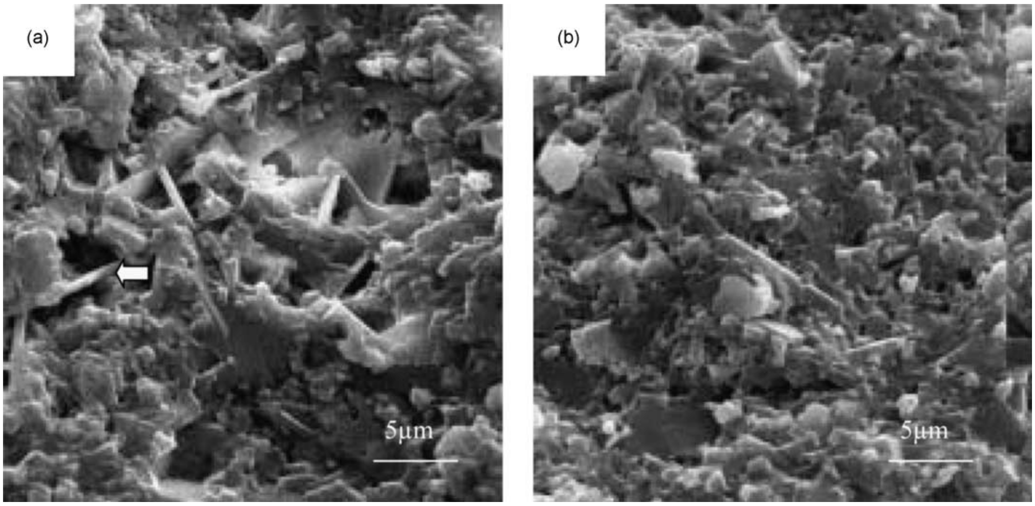

Fig. 3. Fracture surface of as-sintered slag α-sialon samples (a) PLS at 1800 °C for 2 h (b) HP at 1700 °C for 1 h.

1800 °C for 2 h respectively. The etched microstructures of PLS and HP samples are shown in Fig. 2. Some elongated or plate-like grains can be found in both of them, but these types of grains are coarser in the PLS sample. This can be attribute to its higher sintering temperature and more porous for grain growth. The starting slag α-sialon powders are around 1 μm and have an equi-axed morphology, so it can be concluded that these coarse elongated or plate-like grains formed by ostwald growth during sintering. This supports the findings that the morphology of grains after sintering is mainly attributed to their crystal habit and grain growth space.[7]

The density and mechanical properties of the HP and PLS sintered samples are presented in Table 1. The theoretical density of slag α-sialon is 3.19 g/cm^3, obtained by measuring the density of the slag α-sialon powder. Hence, the HP sample attained a bulk density of >99% and PLS samples achieved a bulk density of 96% of the true density. It is also seen in Table 1 that the strength of the HP sample reached 599 MPa and the hardness and toughness of PLS sample were 15.53 GPa and 4.72 MPam$^{1/2}$. These properties are very close to that of normal α-sialon ceramics prepared using very expensive chemical starting powders. Although the HP sample is dense, the hardness is lower than normal HP α-sialons (generally above 18 GPa). This might be attributed to the presence more glass at grain boundaries, which is soft and brittle. The lower strength of PLS sample is related to its low density and weak bonding between grains. The fracture surface of samples (shown in Fig. 3) further indicates that the large

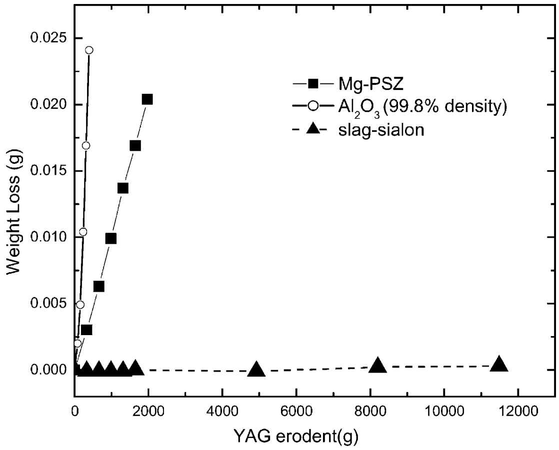

Fig. 4. Cumulative weight loss of samples as a function of the amount of YAG erodent impinging on the target surface at 90-degree angle.

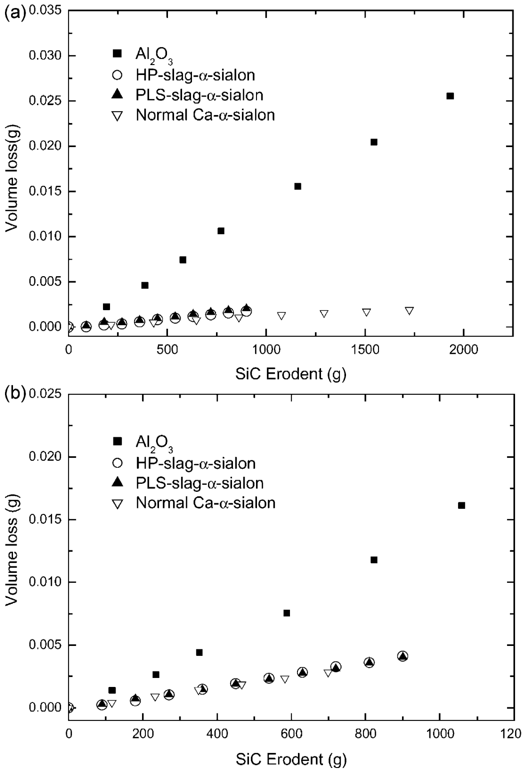

Fig. 5. Cumulative volume loss of samples as a function of the amount of SiC erodent impinging on the target surface at (a) 30-degree angle (b) 90-degree angle.

pores and some big plate-like grains (indicated by an arrow) impair its strength greatly (generally above 500 Mpa) in PLS slag α-sialon. Some grain pullout (indicated by arrows) can be observed in the dense HP salg α-sialon sample, which should lead to reinforcement and thus strength.

3.2. Erosion resistance

Figs. 4 and 5 present the cumulative weight or volume loss due to erosion of the ceramic samples as a function of the amount of YAG or SiC erodent impinging on the material surface. For comparison, Al_2O_3, ZrO_2 and a normal PLS Ca-α-sialon ceramic were also tested. The properties of these reference samples are listed in Table 2. As can be seen, in the case of erosion using YAG erodent at a 90-degree angle, Al_2O_3 and ZrO_2 ceramics show much higher rate of erosive loss than the as-sintered PLS slag-sialon ceramics. When using the harder SiC erodent particles at 30 and 90°, both the HP and PLS sintered slag α-sialon samples were much better than the Al_2O_3 ceramics, and very close to normal α-sialon ceramics prepared using high purity powders. It can also be seen that the erosion rates of all target materials impinged at 30° are lower than that at 90°. This difference can be attributed to different material removal mechanisms in these two cases. In the case of shallow angle eroded surface, the dominant materials removal mechanism was grain ejection and plastic deformation, while in the case of the high angle eroded surface, the material removal mechanism was mainly grain ejection. Figs. 6 and 7 show the representative surface features of slag α-sialon after erosion using SiC erodent at 30 and 90° impacts. In Figs. 6(a) and 7(a), obvious plastic smearing can be observed and in Figs. 6(b) and 7(b), more grain ejection effects can be

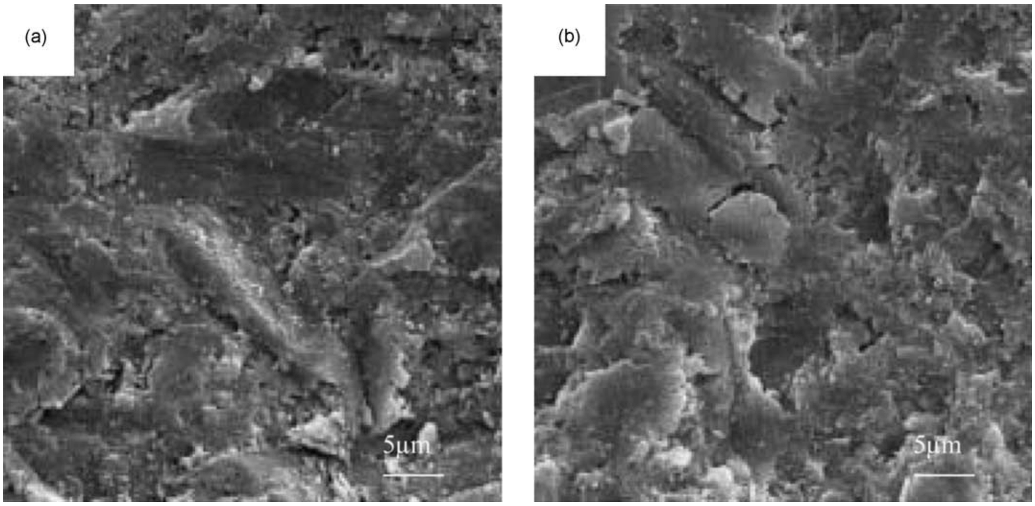

Fig. 6. SEM micrographs of surface features of PLS slag-sialon samples after erosion using SiC particles at impingement angle of (a) 30° and (b) 90°.

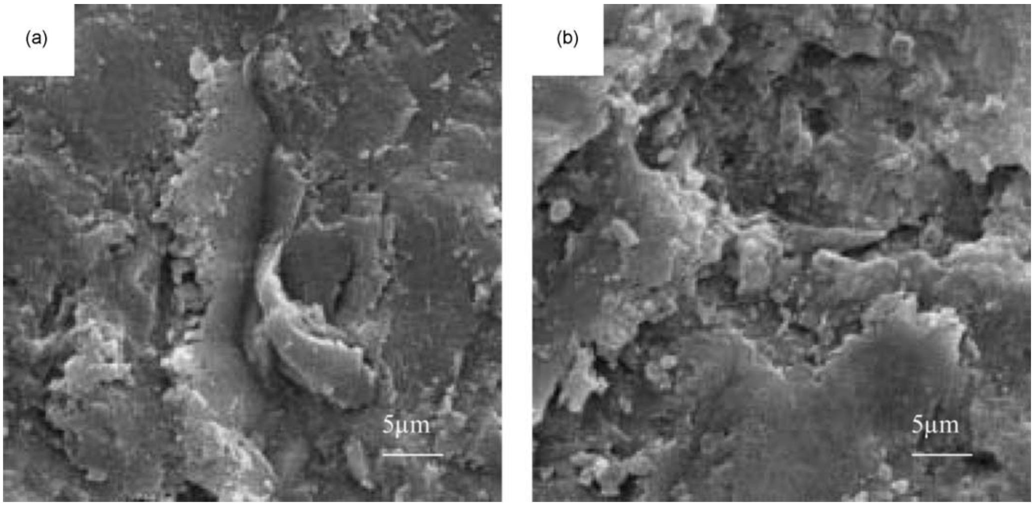

Fig. 7. SEM micrographs of surface features of HP slag α-sialon samples after erosion using SiC particles at impingement angle of (a) 30° and (b) 90°.

noticed. At low angle impact, the kinetic energy of the impinging particles contributes mainly to the ploughing mechanism and very little to normal repeated impact. At high angle impact, the kinetic energy of the impinging particles contributes mainly to repeated impact. The ploughing mechanism is associated with the plastic smearing and cutting of the materials, while the repeated impact mechanism is responsible for initiating and propagating grain boundary microcracks.[8] Ceramics have high hardness and low toughness, and thus they are not easily plastically deformed, but cracks readily propagate to form a crack network. Therefore, the material removal rate is low at low angle impact and high at high angle impact. In addition, because there is not much difference in hardness and toughness between HP and PLS slag α-sialon samples, the erosion-resistance is similar in these two cases.

4. Conclusions

The α-sialon powder synthesized by SHS from slag displays properties suitable for the preparation of ceramic products. The as-sintered slag α-sialon samples showed good mechanical properties very close to that of normal expensive α-sialon ceramics, and a much better erosion resistance than that of ZrO_2 and Al_2O_3 ceramics. Because of the low cost of this process and the starting materials, future applications of the material by industry are therefore anticipated.

Acknowledgements

This work was supported by National Natural Sciences Foundation of China, the Outstanding Overseas Chinese Scholars Fund of Chinese Academy of Sciences and Monash University, Australia.

References

1. Chen, W. W., Wang, P. L., Chen, D. Y. *et al.* Synthesis of (Ca, Mg)-α-sialon from slag by self-propagating high-temperature synthesis. *J. Mater. Chem.*, 2002, **12**, 1199–1202.
2. Ekström, T. and Nygren, M., Sialon ceramics. *J. Am. Ceram. Soc.*, 1992, **75**, 259–276.
3. Bonazza, A., Cunico, L., Dircetti, G., Dondi, M., Guarini, G. and Ruffini, A., Recycling of steel slag in clay brick production. *Key Engineering Materials*, 2002, **206–213**, 835–838.
4. Ovecoglu, M. L., Microstructural characterization and physical properties of a slag-based glass-ceramic crystallized at 950 and 1100 °C. *J. Eur. Ceram. Soc.*, 1998, **18**, 161–168.
5. Ekström, T., Shen, Z. J., Mackenzie, K. J. D., Brown, I. W. M. and White, G. V., α-sialon ceramics synthesised from a clay precursor by carbothermal reduction and nitridation. *J. Mater. Chem.*, 1998, **4**, 977.
6. Zhang, Y., Cheng, Y. B. and Lathabai, S., Erosion of alumina ceramics by air- and water-suspended garnet particles. *Wear*, 2000, **241**, 40–51.
7. Chen, W. W., Sun, W. Y., Wang, P. L., Li, Y. W., Cheng, Y. B. and Yan, D. S., Control of microstructures in α-sialon ceramics. *J. Am. Ceram. Soc.*, 2002, **85**, 276–278.
8. Zhang, Y., Cheng, Y. B. and Lathabai, S., Influence of microstructure on the erosive wear behavior of Ca α-sialon materials. *J. Eur. Ceram. Soc.*, 2001, **21**, 2435–2445.